HHS Public Access

Author manuscript

J Immunol. Author manuscript; available in PMC 2021 January 01.

Published in final edited form as:

J Immunol. 2020 January 01; 204(1): 137–146. doi:10.4049/jimmunol.1900721.

Diacylglycerol kinase ζ regulates macrophage responses in juvenile arthritis and cytokine storm syndrome mouse models

Sahil Mahajan[1], **Elizabeth D. Mellins**[2], **Roberta Faccio**[1,3,*]

[1]Department of Orthopaedic Surgery, Musculoskeletal Research Center, Washington University School of Medicine, St. Louis, MO, USA

[2]Depatment of Pediatrics, Program in Immunology, Stanford University, Stanford, CA, USA

[3]Shriners Hospitals for Children, St. Louis MO

Abstract

Dysregulation of monocyte and macrophage responses are often observed in children with systemic juvenile idiopathic arthritis (sJIA) and cytokine storm syndrome (CSS), a potentially fatal complication of chronic rheumatic diseases. Both conditions are associated with activation of Toll Like Receptor (TLR) signaling in monocyte and macrophage lineage cells, leading to overwhelming inflammatory responses. Despite the importance of TLR engagement in activating pro-inflammatory macrophages, relatively little is known about activation of intrinsic negative regulatory pathways to attenuate excessive inflammatory responses. Here we demonstrate that loss of diacylglycerol kinase ζ (*Dgkζ*), an enzyme which converts diacylglycerol (DAG) into phosphatidic acid (PA), limits inflammatory cytokine production in an arthritic mouse model dependent on TLR2 signaling and in a CSS mouse model dependent on TLR9 signaling. *In vitro Dgkζ* deficiency results in reduced production of TNFα, IL-6 and IL-1β, and limited M1 macrophage polarization. Mechanistically, *Dgkζ* deficiency decreases STAT1 and STAT3 phosphorylation. Moreover, Dgkζ levels are increased in macrophages derived from mice with CSS or exposed to plasma from sJIA patients with active disease. Our data suggest that *Dgkζ* induction in arthritic conditions perpetuates systemic inflammatory responses mediated by macrophages and highlight a potential role of *Dgkζ*-DAG/PA axis as a modulator of inflammatory cytokine production in sJIA and CSS.

Introduction

Systemic juvenile idiopathic arthritis (sJIA) is a multifactorial inflammatory disease that can exhibit bone and joint damage along with various non-articular symptoms, such as fever, rash and serositis, including pericarditis and pleuritis (1, 2). A critical aspect of sJIA is its association with a life-threatening condition called cytokine storm syndrome (CSS) (3, 4); CSS is characterized by overwhelming production of inflammatory cytokines by activated T cells and macrophages, leading to multi-organ failure (5–9). Unfortunately, the causes of sJIA and CSS remain to be fully established.

*Correspondence should be addressed to: Roberta Faccio, Box 8233, 425 S. Euclid, St. Louis, MO 63110, USA, Phone: 314-747-4602, Fax: 314-362-0334, faccior@wustl.edu.

A critical driver of sJIA is aberrant activation of innate immune cells of the monocytic/macrophage lineage, while defective T cell cytotoxic pathways have been associated with CSS following viral infections. However, the presence of activated monocytes and macrophages in the circulation and peripheral organs, and elevated levels of pro-inflammatory cytokines produced by monocytes/macrophages have also been observed in sJIA patients developing CSS (10–13). Microarray studies performed on peripheral blood mononuclear cells (PBMC) obtained from untreated sJIA patients indicated enrichment of genes linked with monocyte/macrophage activation, in particular those associated with Toll Like Receptor (TLR) signaling, in the subset of patients with high ferritin levels, a marker associated with development of CSS (14). Polymorphism in interferon regulatory factor 5 (IRF5), a molecule activated in response to TLR signaling and associated with macrophage activation, has been reported in sJIA patients with CSS (15). IRF5 is also involved in the differentiation of specialized macrophages called hemophagocytes that phagocytose blood elements leading to anemia and thrombocytopenia in CSS. Interestingly, cell intrinsic TLR7/9 signaling is required for the differentiation of hemophagocytes from inflammatory monocytes in mice (16). Recent data, including from our laboratory, demonstrated that depletion of monocytes and macrophages ameliorates CSS progression in two murine models, one dependent on defective T cell cytolytic pathways following a viral infection and a second on repetitive stimulation of TLR9 signaling (17). Inappropriate activation of TLRs in macrophages is also reported in rheumatoid arthritis (RA), type 2 diabetes, systemic lupus erythematous and other diseases associated with systemic inflammation (18, 19). However, what drives the persistent TLR signaling in monocytes/macrophages and why intrinsic negative regulatory pathways fail to keep the overwhelming inflammatory responses in check remain to be addressed.

Diacylglycerol (DAG) is a key second messenger that controls a variety of cellular processes and acts as the substrate for the synthesis of various lipid molecules (20, 21). In myeloid cells, ligation of TLRs leads to the generation of DAG suggesting that its levels might be tightly controlled to coordinate TLR signaling (22, 23). DAG levels in the cells are rapidly regulated by a class of enzymes called diacylglycerol kinases (Dgks). Dgks selectively catalyze the phosphorylation of DAG to generate phosphatidic acid (PA), thus ceasing the processes that depends upon DAG and initiating PA-dependent regulatory pathways. Mammals express ten isoforms of Dgk, each with its ability to respond to multiple intracellular and extracellular signals. Despite their sheer number, each member shows functional selectivity, specific tissue distribution and subcellular localization (24–26). We have previously demonstrated that Dgkζ is the most prominent isoform expressed in macrophages and osteoclasts, a bone resorptive cell type derived from the monocyte-macrophage lineage (27). Dgkζ levels are further elevated in the macrophages upon exposure to LPS (28). Further advances indicating the importance of DAG signaling have emerged from mouse models that involve ablation of Dgkζ. *Dgkζ* deficient mice show an osteoporotic bone phenotype due to the increased number of osteoclasts (27). Loss of *Dgkζ* also results in hyper-responsive T cells with increased cytokine production upon T cell receptor stimulation (29). These results suggest that Dgkζ activation drives intrinsic negative regulatory mechanisms that downregulate pro-inflammatory responses through the conversion of DAG into PA. In this paper, we tested the hypothesis that DAG signaling is

required for monocyte and macrophage activation; we predicted that *Dgkζ*-/- mice would have increased susceptibility to systemic inflammation driven by activated macrophages. To our surprise, however, we observed that loss of *Dgkζ* significantly reduces the severity of inflammatory arthritis in a TLR2-dependent mouse model and cytokine production in TLR9-induced CSS. Mechanistically, macrophages derived from *Dgkζ* deficient animals have abated responses to TLR ligands and impaired M1 macrophage polarization. The defective pro-inflammatory cytokine secretion and increased DAG accumulation in *Dgkζ* deficient macrophages contribute to reduced phosphorylation of STAT1 and STAT3. Our results indicate that *Dgkζ* induction in arthritic conditions perpetuates macrophage-dependent systemic inflammatory responses and highlight a potential role for Dgkζ-DAG/PA axis in sJIA and CSS.

Materials and Methods:

Mice

Dgkζ-/- mice were kindly provided by Dr. Gary A. Koretzky (Weill Cornell Medical College, New York, NY) and maintained by homozygous breeding. Mice were housed in cages and were fed with food and water ad libitum, with a 12-hour light and 12-hour dark cycle. All experiments were approved by the Washington University School of Medicine animal care and use committee.

Induction of streptococcal cell wall (SCW) arthritis

SCW arthritis was induced into 6 to 8 week old WT and *Dgkζ-/-* mice by a single intraarticular injection of 25 μg of SCW preparation (peptidoglycan-polysaccharide 100p fraction; Lee laboratories, Grayson, GA, USA) into the right ankle joint of naive mice. Injection of PBS into the left ankle joint served as a control. Ankle swelling was measured daily by blinded investigators using a caliper. Animals were sacrificed 3 days after SCW delivery.

CpG-induced model of CSS

6 to 8 week-old male or female WT and *Dgkζ-/-* mice were given 50 μg of CpG 1826 (IDT) intraperitoneally on days 0, 2, 4, 6 and 8. On day 9, animals were bled via submandibular vein puncture for complete blood count and euthanized to collect liver for FACS and histological analysis.

Histology

For the SCW mouse model, both the PBS and SCW injected joints were isolated, fixed in 10% buffered formalin phosphate (Fisher Scientific) and decalcified using Immunocal (StatLab) for 3 days. The joints were embedded in paraffin wax and stained with hematoxylin and eosin (H&E). The joint samples were additionally stained with safranin O. Livers from the TLR9 injected mice were fixed with 10% buffered formalin phosphate. The samples were embedded in paraffin before being cut into 5 μM sections and stained with H&E. Images were acquired using a Nikon Eclipse 80i microscope equipped with a Nikon DS-Fi1 camera and NIS-Elements BR3.2 software (Nikon, Japan). The severity of inflammation in the liver was determined by assessing the presence of inflammatory

infiltrates around the veins and within the parenchyma and scored on a scale of 0–4 with 0 being no inflammatory infiltrates and 4 being maximal presence of inflammatory infiltrates.

Primary cell cultures

Bone marrow isolated from tibias and femurs of WT and *Dgkζ-/-* was cultured in alpha-MEM containing 10% heat-inactivated fetal bovine serum, 100 IU/ml penicillin, 100 μg/ml streptomycin, glutamine (α−10 medium), and 1/10 vol CMG14–12 cell-conditioned medium (30) as a source of MCSF, for 7 days to obtain bone marrow derived macrophages (BMMs). BMMs were treated with 100 ng/ml of LPS (Sigma), 40 μg/ml of poly (I:C), 50 ng/ml of pam3CSK4 (InvivoGen), 1 μl/ml of BD GolgiPlug (BD), 100 nM PMA, 100 ng/ml IFNγ or 50 ng/ml of IL-4 for the indicated time points and subjected to either western blot analysis or RT-PCR for markers of M1 and M2 macrophage polarization.

SDS-PAGE and immunoblot analysis

WT and *Dgkζ-/-* BMMs treated with 100 ng/ml LPS, 100ng/ml IFNγ or 50 ng/ml IL-4 for the indicated time points were lysed in RIPA buffer (20 mM Tris-HCl, pH 7.5, 150 mM NaCl 1 mM EDTA, 1 mM EGTA, 1% Nonidet P-40, 1% sodium deoxycholate) supplemented with protease/phosphatase inhibitor cocktail (Pierce). The protein lysates were resolved by SDS-PAGE and electro-transferred into nitrocellulose membranes and probed with specific antibodies. The following antibodies were used: phospho-STAT1 (7649, Cell Signaling Technology), STAT1 (9172, Cell Signaling Technology), phospho-STAT3 (9145, Cell Signaling Technology), STAT3 (4904, Cell Signaling Technology), phospho-STAT6 (9361, Cell Signaling Technology), STAT6 (5397, Cell Signaling Technology), phospho-AKT (4060, Cell Signaling Technology), AKT (2966, Cell Signaling Technology), phospho-p38 MAPK (9216, Cell Signaling Technology), p38 MAPK (9219, Cell Signaling Technology), phospho-GSK3β (9336, Cell Signaling Technology), GSK3β (9315, Cell Signaling Technology) and β-Actin (A5441, Sigma).

Measurement of cytokine, ferritin and nitrite levels

Cytokine levels in the serum of mice with TLR9-induced CSS or in BMM culture supernatants were quantified using ELISA kits specific for IL-6, TNFα and IL-1β (eBioscience). The serum ferritin levels was determined by ferritin mouse ELISA kit purchased from Abcam and nitrite levels in BMM culture supernatant were determined by Griess reagent kit (Molecular Probes) as per the manufacturer's protocols.

RNA and real-time PCR analysis

RNA was isolated from BMMs cultured *in vitro* or from livers of mice with TLR9-induced CSS using RNeasy Mini Kit (Qiagen). Purified RNA was then reverse transcribed to cDNA using High Capacity cDNA reverse transcription kit (Applied Biosystems) according to the manufacturer's instructions. The subsequent real-time PCR analysis was performed with SYBR Green PCR Master Mix (Applied Biosystems) and primers specific for murine Dgkζ, IL-1β, IL-6, TNF-α, iNOS, CCL5, IRF5, Arginase 1, PPARγ, TLR4, CD14 and cyclophilin were used as follow: for Dgkζ, ATGCTGGGACGGCCTTCT (forward) and TCGGATGTGCTTGGCTAAGTC (reverse); IL-1β, GCTTCCTTGTGCAAGTGTCTGA

(forward) and TCAAAAGGTGGCATTTCACAGT (reverse); IL-6, TTCTCTGGGAAATCGTGGAAA (forward) and TGCAAGTGCATCATCGTTGTT (reverse); TNFα, CTGTAGCCCACGTCGTAGC (forward) and TTGAGATCCATGCCGTTG (reverse); iNOS, ACTCAGCCAAGCCCTCACC (forward) and GCCTATCCGTCTCGTCCGT (reverse); CCL5, AGATCTCTGCAGCTGCCCTCA (forward) and GGAGCACTTGCTGCTGGTGTAG (reverse); IRF5, TGTCCCAGACCCAAATCTCC (forward) and CTCTAGGTCCGTCAAAGGCA (reverse); Arginase 1, ATGGAAGAGACCTTCAGCTAC (forward) and GCTGTCTTCCCAAGAGTTGGG (reverse); PPARγ, ACTCATACATAAAGTCCTTCCCGCT (forward) and ATGGTGATTTGTCCGTTGTCTTTCC (reverse); TLR4, GGCAGCAGGTGGAATTGTAT (forward) and TGCCGTTTCTTGTTCTTCCT (reverse); CD14, CTGATCTCAGCCCTCTGTCC (forward) and CCCGCAGTGAATTGTGACTA (reverse) and for cyclophilin AGCATACAGGTCCTGGCATC (forward) and TTCACCTTCCCAAAGACCAC-3' (reverse).

Statistics

All data represent mean and SD. For statistical comparisons, data were analyzed using two-tailed Student's t test. All experiments with multiple comparisons were analyzed by a one-way or two-way analysis of covariance in conjunction with a Bonferroni post-hoc test. For survival studies, the significance was determined by log-rank test. P value of <0.05 was set as statistically significant, *$p<0.05$ **$p<0.01$, ***$p<0.001$.

Results

Dgkζ deficient mice are protected from streptococcal cell wall (SCW)-induced arthritis

To address the importance of *Dgkζ* signaling in modulating macrophage responses in arthritic conditions, we injected the right ankle of WT and *Dgkζ* null mice with 25 μg of SCW fragments to induce a local inflammatory response associated with bone and cartilage disruption subsequent to macrophage infiltration. As control, the contralateral ankle was injected with PBS. Three days later, WT mice developed significant swelling in the SCW-injected ankle compared to the contralateral leg. Based on the hyper-active T cell (29) and osteoclast phenotypes (27) known to result from *Dgkζ* deficiency, we expected *Dgkζ* null animals to develop more severe inflammation than WT mice. Surprisingly, however, *Dgkζ* deficient mice exhibited significant less swelling, as shown by the reduced ankle thickness and redness compared to WT mice (Fig. 1A). Histological analysis of H&E stained sections showed significant immune infiltration and tissue destruction in the SCW-injected ankle of WT mice (Fig. 1B). Interestingly, despite presence of inflammatory infiltrates, *Dgkζ* null mice were protected from joint and cartilage disruption, as shown by the intact safranin-O staining (Fig. 1C). To assess the cellular composition of the immune infiltrates in the ankle joints of WT and *Dgkζ* null mice, we performed RT-PCR on the snap-frozen ankles 3 days after the intra-articular injection of SCW fragments. We found elevated levels of CD11b, a myeloid cell marker expressed in monocytes, and significant upregulation of F4/80, a specific macrophage marker, in the SCW-injected ankles of WT and *Dgkζ* null mice compared to the contralateral leg injected with PBS. No changes in the levels of CD3, a T

cell marker, were observed between the SCW and PBS-injected ankles of both WT and *Dgkζ* null mice (Fig. 1D). To assess whether the reduced swelling and tissue disruption observed in the knockout mice was due to aberrant production or secretion of inflammatory cytokines, we measured the expression of IL-6, TNFα and IL-1β transcripts in the ankles isolated from WT and *Dgkζ*-/- mice. Strikingly, we observed significantly lower levels of these pro-inflammatory cytokines in the SCW-injected ankles from *Dgkζ*-/- mice compared to WT (Fig. 1E). No significant differences were observed in the control ankles (Fig. 1E). These results suggest that *Dgkζ* mediated signaling is critical for macrophage responses and that, unlike for T cells and osteoclasts, *Dgkζ* loss reduces inflammatory cytokine production by monocytes/macrophages.

Dgkζ deficiency attenuates CSS development

To further assess the importance of *Dgkζ* signaling in macrophage activation *in vivo*, we turned to CSS, a severe and potentially fatal complication occurring in patients with chronic rheumatic conditions such as sJIA and characterized by the overwhelming production of pro-inflammatory cytokines. The repeated administration of the TLR9 ligand, CpG (50 μg), provides a macrophage-dependent model to study CSS (17, 31). To address whether *Dgkζ* knockout mice were protected from TLR9-induced CSS, *Dgkζ* deficient and WT mice received CpG injections every other day for 8 days and were sacrificed on day 9. As reported previously, WT mice injected with CpG developed splenomegaly, hepatomegaly and a significant decrease in white blood cell (WBC) and platelet counts compared to PBS injected controls (Fig. 2A-E). A similar increase in the spleen and liver weight, as well as decrease in WBC counts were observed in *Dgkζ-/-* mice receiving CpG (Fig. 2A-E). Furthermore, H&E-stained liver sections revealed comparable areas of inflammatory infiltrates (Fig. 2G, 2H) and percentage of $F4/80^{+}CD11b^{+}$ liver macrophages (Fig. 2I) in both genotypes following CpG injections. Strikingly, however, serum ferritin levels, a marker of liver damage, and IL-1β, IL-6 and TNFα mRNA levels from the livers of *Dgkζ-/-* mice were significantly lower than in WT animals (Fig. 2F, 2J). Consistent with this observation, IL-6 serum levels were also significantly decreased in *Dgkζ-/-* animals injected with CpG versus WT (Fig. 2K). These results suggest that *Dgkζ* deficiency, while not affecting tissue infiltration by monocytes/macrophages, reduces the production of inflammatory cytokines and limits liver damage *in vivo* in the TLR9-induced CSS model.

Loss of *Dgkζ* limits pro-inflammatory cytokine production following TLR engagement

To investigate whether the reduced pro-inflammatory cytokine levels in the SCW arthritis and TLR9-induced CSS observed in *Dgkζ* deficient mice were due to hypo-responsiveness of the macrophages to TLR signaling, we stimulated WT and *Dgkζ-/-* bone marrow derived macrophages (BMMs) with 100 ng of LPS, a TLR4 ligand, *in vitro*. Confirming the *in vivo* observations, we observed significantly reduced transcript levels of IL-6, TNFα and IL-1β in *Dgkζ-/-* BMMs compared to WT (Fig. 3A). Consistently, *Dgkζ-/-* BMMs secreted significantly lower levels of pro-inflammatory cytokines compared to WT BMMs as determined by ELISA (Fig. 3B). Importantly, the impaired response to LPS was not due to reduced expression of the LPS cognate receptors TLR4 or CD14 (not shown). Indeed, reduced IL-6, TNFα and IL-1β transcripts in *Dgkζ-/-* BMMs were also observed upon activation of TLR3 with poly (I:C) or TLR2 with Pam3CSK4 (Fig. 3C, 3D). Consequently,

IL-6 and TNFα secretion in the culture supernatant were reduced in response to Pam3CSK4 or CpG treatments (Fig. 3E, F). These findings show that *Dgkζ* is necessary for pro-inflammatory cytokine production by activated macrophages following TLR engagement.

Dgkζ deficient macrophages have reduced STAT1/3 phosphorylation

To understand the mechanisms by which loss of *Dgkζ* limits inflammatory cytokine production, we turned to signaling pathway activated downstream of TLRs and known to modulate cytokine production by macrophages (32, 33). We have previously demonstrated that *Dgkζ*-/- BMMs have higher levels of DAG isoforms containing both saturated and unsaturated fatty acids compared to WT (27), consistent with the known role of this kinase in converting DAG into PA. PI3K/AKT pathway has also been shown to be increased in *Dgkζ*-/- cells (28), however, we did not detect differences in AKT phosphorylation between WT and *Dgkζ*-/- BMMs following stimulation with LPS (Supplemental Fig. 1A). We also did not observe any difference in the phosphorylation of GSK3β, a downstream target of AKT (not shown). Similarly, p38 MAPK, pERK and pIκBα, known pathways modulating cytokine production, were unchanged between the two genotypes (Supplemental Fig. 1B and not shown). In contrast, we observed that the phosphorylation of STAT1 and STAT3 was significantly decreased in *Dgkζ-/-* BMMs stimulated with LPS compared with WT (Fig. 4A, 4B). Next, to determine whether reduced STAT1/3 phosphorylation in *Dgkζ-/-* BMMs was due to elevated DAG levels, we treated WT BMMs with 100 nM of the non-hydrolyzable DAG analog PMA during the 1 or 2 hour stimulation with LPS. pSTAT1 and pSTAT3 levels were significantly reduced in WT cells exposed to PMA, suggesting DAG accumulation as a potential mechanism for reduced STAT signaling (Fig. 4C, 4D). Because *Dgkζ-/-* BMMs produced less inflammatory cytokines, which in turn could activate STAT signaling in an autocrine manner, we incubated the cells with 1 μl/ml of GolgiPlug, a protein transport inhibitor that blocks cytokine secretion. STAT1 and STAT3 phosphorylation was reduced by GolgiPlug in LPS treated BMMs derived from both WT and *Dgkζ-/-* mice (Fig. 4E, 4F). In contrast, similar levels of STAT1 phosphorylation were observed in both WT and *Dgkζ-/-* BMMs upon IFNγ treatment (Supplemental Fig. 1C). These results indicate that Dgkζ loss impacts STAT1/3 activation downstream of the LPS/TLR4 pathway via intrinsic (DAG accumulation) and extrinsic (reduced cytokine secretion) mechanisms.

Dgkζ deficient macrophages have impaired M1 macrophage polarization

Because STAT1/3 signaling modulates M1 macrophage polarization, next we monitored the expression of genes that are hallmarks of M1 pro-inflammatory macrophages. We observed that *Dgkζ*-/- BMMs expressed lower levels of iNOS, CCL5 and IRF5 upon LPS stimulation compared to WT cells (Fig. 5A). The decrease in iNOS also correlated with lower levels of NO released in the supernatant of *Dgkζ-/-* BMMs compared to WT following activation with LPS and IFNɣ (Fig. 5B). In contrast, IL-4 treatment to induce M2 polarization resulted in a similar activation of p-STAT6 and comparable induction of Arginase 1 and PPARɣ expression in both genotypes (Fig. 5C, 5D). These data indicate that loss of *Dgkζ* in macrophages limits their polarization to a M1 macrophage pro-inflammatory state.

Dgkζ levels are increased in arthritic conditions

Finally, we analyzed Dgkζ levels in macrophages *in vitro* in response to inflammatory stimuli or after exposure to plasma from sJIA patients and *ex-vivo* in livers from mice with TLR9 induced CSS. We observed that Dgkζ levels were increased in response to TLR ligands LPS and CpG, whereas no changes in its expression occurred after IL-4 stimulation (Fig. 6A). We also found higher Dgkζ levels in liver extracts of WT mice that were given repeated CpG injections to induce CSS compared to WT mice that received PBS (Fig. 6B). Importantly, macrophages exposed to plasma from sJIA patients with active disease had significantly higher levels of Dgkζ compared to cells exposed to healthy control plasma (Fig. 6C). Collectively, these data indicate that under inflammatory conditions Dgkζ expression is increased to support M1 macrophage polarization.

Discussion

In this study, we determined the role of *Dgkζ* in modulating macrophage pro-inflammatory responses. *Dgkζ* deficient mice have defective macrophage polarization to an M1 pro-inflammatory phenotype, and therefore are protected from joint damage in the SCW model of arthritis and from mounting an overwhelming cytokine storm in the TLR9-induced CSS. Our data argue that Dgkζ deletion induces macrophage hypo-responsiveness to TLR signaling and limits M1 macrophage activation, thus highlighting the importance of *Dgkζ*-DAG/PA axis in autoimmune and inflammatory diseases driven by macrophages.

Macrophages are critical players in inflammatory diseases because of their capacity in both commencing and terminating inflammatory responses. Macrophages are highly plastic cells, sensitive to their microenvironment, with the ability to polarize to an “M1-like” pro-inflammatory phenotype in response to LPS and/or IFNɣ, and to an “M2-like” anti-inflammatory phenotype in response to IL-4 and tissue damage (34, 35). The relative contribution of M1 and M2 macrophage populations in systemic inflammatory disorders including RA is not well understood. In the K/BxN serum transfer model of inflammatory arthritis, $Ly6C^-$ monocytes recruited to the affected joints are converted into classically activated macrophages during the effector phase of arthritis. The same population is then polarized to an M2 macrophage phenotype during later stages of arthritic progression (36). Similarly, peripheral blood mononuclear cells from sJIA patients present a mixed M1 and M2 macrophage phenotype (37). However, in malignancies, M1 and M2 macrophages have been shown to derive from cells of different origin, with the pro-inflammatory subsets originating from hematopoietic stem cells in the bone marrow and the anti-inflammatory subsets from tissue resident embryonic precursors (38). With the use of single cell RNA sequencing approaches, several macrophage subsets distinct from the classical M1 and M2 polarization status, have been discovered (39, 40). In RA synovial tissues, Kuo and colleagues identified a new macrophage subset, characterized by the expression of heparin-binding EGF-like growth factor (HBGEF). This subset promotes fibroblast invasiveness, thus contributing to pannus-associated tissue destructive behaviors in arthritic joints (40).

We find that macrophages from *Dgkζ-/-* mice have reduced M1 markers and decreased production of pro-inflammatory cytokines in response to M1 polarizing factors and in the TLR-dependent models of arthritis and CSS. In contrast, acquisition of M2 markers

following exposure to IL-4 does not appear to be affected by *Dgkζ* deficiency. Consistent with this phenotype, phosphorylation of STAT1 and STAT3, M1 specific pathways, but not STAT6, which is involved in M2 polarization, are modulated by *Dgkζ*. Modulation of STAT1/3 activation by *Dgkζ* deficiency appears to occur downstream of the LPS/TLR4 pathway but not IFNɣ signaling. Furthermore, while *Dgkζ* loss is sufficient to decrease macrophage-mediated pro-inflammatory cytokine production *in vivo*, it does not prevent the recruitment of inflammatory cells in the tissues in both SCW arthritis and CSS. Further analysis is required to determine whether *Dgkζ* loss represents a distinct macrophage subset with reduced ability to respond TLR ligands, yet incapable of mounting anti-inflammatory responses.

We previously reported that loss of *Dgkζ* in BMMs leads to increased expression of c-Fos, a transcription factor known to be involved in osteoclast differentiation (27). *Dgkζ*-/- BMM cultures have the ability to form more osteoclasts than WT when exposed to a pro-osteoclastogenic milieu (27). Thus, it is plausible that accumulation of DAG at the expense of PA in the monocyte/macrophage lineage cells drives the pro-osteoclastogenic machinery at the expense of activating pro-inflammatory signals. This assumption is further supported by the observation that DAG signaling activates PKC-mediated pathways required for osteoclast formation and bone resorption (41, 42). In contrast, PA has been reported to be required for inflammatory cytokine production. Administration of PA restores IL-12 production in *Dgkζ* deficient macrophages in vitro and increases serum cytokine levels when delivered into mice (28, 43). At present, however, is not completely clear whether *Dgkζ* deficiency alters macrophage activation through accumulation of DAG or inadequate PA levels or both. Adding to the complexity, both DAG and PA levels are increased in response to inflammatory stimuli. DAG is induced in macrophages within minutes following LPS stimulation (22, 23) and PA accumulates immediately after stimulation with zymosan (44). We find that treatment of WT macrophages with the non-hydrolyzable DAG analog PMA limits the phosphorylation of STAT1 and STAT3 upon LPS treatment, suggesting that increased DAG levels can control macrophage activation. However, we also find that blocking inflammatory cytokine secretion in LPS-activated macrophages reduces STAT1/3 phosphorylation, suggesting that extrinsic factors, in addition to increased DAG levels, could act in an autocrine manner to modulate *Dgkζ-/-* macrophage responses. Interestingly, however, stimulation with IFNγ does not lead to differences in STAT signaling between WT and *Dgkζ-/-* macrophages, thus implying that Dgkζ might preferentially modulate signaling downstream of TLRs.

Dgkζ expression is not solely confined to monocyte/macrophages, and immune imbalances due to the effects of *Dgkζ* loss have been described in T cells, mast cells and DCs. In T cells, Dgkζ inhibits DAG mediated T cell receptor signaling and T cell activation while promoting T cell anergic responses (29, 45). In mast cells, depending upon the context, Dgkζ can either activate FceR1-mediated responses to promote degranulation or inhibit IL-6 production (46). In dendritic cells, Dgkζ induces cytokine production by inhibiting PI3K activity (28). Thus, aberrant activation of additional immune populations other than macrophages might be contributing to the fact that *Dgkζ-/-* mice are not fully protected from CSS and develop hepatosplenomegaly and pancytopenia. These findings also highlight the

complexity of Dgkζ signaling in immune cells and how its effects are cell type-specific and/or dictated by extracellular signals.

The enzymatic activity of phospholipases leads to the generation of DAG and IP3/calcium signaling downstream of TLRs, integrins and receptor tyrosine kinases. We previously reported that PLCγ2-/- mice are protected from development of inflammatory arthritis and CSS due to defective innate immune cell responses, including macrophage mediated inflammatory cytokine production (17, 47). We have also reported that increased in calcium fluxes drive M1 macrophage polarization, leading to more severe development of CSS (17, 48). Intriguingly, both calcium and DAG are generated upon activation of PLCγ2 signaling. Thus, our findings suggest that increased DAG levels could counteract calcium-mediated pro-inflammatory responses, unless promptly converted into PA by the enzymatic activity of *Dgkζ*. Importantly, we find that Dgkζ levels are increased in macrophages upon exposure to inflammatory cytokines, sJIA plasma and in mice with CSS, thus suggesting that blocking Dgkζ upregulation or activity in the macrophages could restore intrinsic negative regulatory signals. In conclusion, our data suggest that *Dgkζ* induction in arthritic conditions perpetuates systemic inflammatory responses mediated by macrophages and highlight a potential role of *Dgkζ*-DAG axis as the driver of inflammatory cytokine production in sJIA and CSS.

Supplementary Material

Refer to Web version on PubMed Central for supplementary material.

Acknowledgments

The authors thank Dr. Biancamaria Ricci, Dr. Zhengfeng Yang, Dr. Won Jong Jin, and Ali Zamani for technical help and suggestions.

This work was supported by R01 AR053628 (RF), R01 AR066551 (RF), R01 AR061297 (EM) from National Institutes of Health (NIH), and Shriners Hospital 85100 (RF) and Siteman Cancer Center to RF. Histological analysis was performed through the Histology Core at the Washington University Musculoskeletal Research Center supported by the P30 grants AR057235 and P30 AR074992

References

1. Bruck N, Schnabel A, and Hedrich CM. 2015 Current understanding of the pathophysiology of systemic juvenile idiopathic arthritis (sJIA) and target-directed therapeutic approaches. Clin Immunol 159: 72–83. [PubMed: 25956529]
2. Petty RE, Southwood TR, Manners P, Baum J, Glass DN, Goldenberg J, He X, Maldonado-Cocco J, Orozco-Alcala J, Prieur AM, Suarez-Almazor ME, Woo P, and R. International League of Associations for. 2004 International League of Associations for Rheumatology classification of juvenile idiopathic arthritis: second revision, Edmonton, 2001. J Rheumatol 31: 390–392. [PubMed: 14760812]
3. Sawhney S, Woo P, and Murray KJ. 2001 Macrophage activation syndrome: a potentially fatal complication of rheumatic disorders. Arch Dis Child 85: 421–426. [PubMed: 11668110]
4. Grom AA, and Passo M. 1996 Macrophage activation syndrome in systemic juvenile rheumatoid arthritis. J Pediatr 129: 630–632. [PubMed: 8917224]
5. Lerkvaleekul B, and Vilaiyuk S. 2018 Macrophage activation syndrome: early diagnosis is key. Open Access Rheumatol 10: 117–128. [PubMed: 30214327]

6. Schulert GS, and Grom AA. 2014 Macrophage activation syndrome and cytokine-directed therapies. Best Pract Res Clin Rheumatol 28: 277–292. [PubMed: 24974063]
7. Jordan MB, Hildeman D, Kappler J, and Marrack P. 2004 An animal model of hemophagocytic lymphohistiocytosis (HLH): CD8+ T cells and interferon gamma are essential for the disorder. Blood 104: 735–743. [PubMed: 15069016]
8. Janka GE 2012 Familial and acquired hemophagocytic lymphohistiocytosis. Annu Rev Med 63: 233–246. [PubMed: 22248322]
9. Das R, Guan P, Sprague L, Verbist K, Tedrick P, An QA, Cheng C, Kurachi M, Levine R, Wherry EJ, Canna SW, Behrens EM, and Nichols KE. 2016 Janus kinase inhibition lessens inflammation and ameliorates disease in murine models of hemophagocytic lymphohistiocytosis. Blood 127: 1666–1675. [PubMed: 26825707]
10. Weaver LK, Chu N, and Behrens EM. 2016 TLR9-mediated inflammation drives a Ccr2-independent peripheral monocytosis through enhanced extramedullary monocytopoiesis. Proc Natl Acad Sci U S A 113: 10944–10949.
11. Nagel M, Schwarting A, Straub BK, Galle PR, and Zimmermann T. 2017 [Hepatic manifestation of a macrophage activation syndrome (MAS)]. Z Gastroenterol 55: 473–478. [PubMed: 28376538]
12. Billiau AD, Roskams T, Van Damme-Lombaerts R, Matthys P, and Wouters C. 2005 Macrophage activation syndrome: characteristic findings on liver biopsy illustrating the key role of activated, IFN-gamma-producing lymphocytes and IL-6- and TNF-alpha-producing macrophages. Blood 105: 1648–1651. [PubMed: 15466922]
13. Canna SW, de Jesus AA, Gouni S, Brooks SR, Marrero B, Liu Y, DiMattia MA, Zaal KJ, Sanchez GA, Kim H, Chapelle D, Plass N, Huang Y, Villarino AV, Biancotto A, Fleisher TA, Duncan JA, O'Shea JJ, Benseler S, Grom A, Deng Z, Laxer RM, and Goldbach-Mansky R. 2014 An activating NLRC4 inflammasome mutation causes autoinflammation with recurrent macrophage activation syndrome. Nat Genet 46: 1140–1146. [PubMed: 25217959]
14. Fall N, Barnes M, Thornton S, Luyrink L, Olson J, Ilowite NT, Gottlieb BS, Griffin T, Sherry DD, Thompson S, Glass DN, Colbert RA, and Grom AA. 2007 Gene expression profiling of peripheral blood from patients with untreated new-onset systemic juvenile idiopathic arthritis reveals molecular heterogeneity that may predict macrophage activation syndrome. Arthritis Rheum 56: 3793–3804. [PubMed: 17968951]
15. Yanagimachi M, Naruto T, Miyamae T, Hara T, Kikuchi M, Hara R, Imagawa T, Mori M, Sato H, Goto H, and Yokota S. 2011 Association of IRF5 polymorphisms with susceptibility to macrophage activation syndrome in patients with juvenile idiopathic arthritis. J Rheumatol 38: 769–774. [PubMed: 21239750]
16. Akilesh HM, Buechler MB, Duggan JM, Hahn WO, Matta B, Sun X, Gessay G, Whalen E, Mason M, Presnell SR, Elkon KB, Lacy-Hulbert A, Barnes BJ, Pepper M, and Hamerman JA. 2019 Chronic TLR7 and TLR9 signaling drives anemia via differentiation of specialized hemophagocytes. Science 363: pii:eaao5213.
17. Mahajan S, Decker CE, Yang Z, Veis D, Mellins ED, and Faccio R. 2019 Plcgamma2/Tmem178 dependent pathway in myeloid cells modulates the pathogenesis of cytokine storm syndrome. J Autoimmun 100: 62–74. [PubMed: 30879886]
18. Ewald SE, and Barton GM. 2011 Nucleic acid sensing Toll-like receptors in autoimmunity. Curr Opin Immunol 23: 3–9. [PubMed: 21146971]
19. Farrugia M, and Baron B. 2017 The Role of Toll-Like Receptors in Autoimmune Diseases through Failure of the Self-Recognition Mechanism. Int J Inflam 2017: 8391230.
20. Hodgkin MN, Pettitt TR, Martin A, Michell RH, Pemberton AJ, and Wakelam MJ. 1998 Diacylglycerols and phosphatidates: which molecular species are intracellular messengers? Trends Biochem Sci 23: 200–204. [PubMed: 9644971]
21. Roberts MF 1994 First thoughts on lipid second messengers. Trends Cell Biol 4: 219–223. [PubMed: 14731681]
22. Zhang F, Zhao G, and Dong Z. 2001 Phosphatidylcholine-specific phospholipase C and D in stimulation of RAW264.7 mouse macrophage-like cells by lipopolysaccharide. Int Immunopharmacol 1: 1375–1384. [PubMed: 11460317]

23. Monick MM, Carter AB, Gudmundsson G, Mallampalli R, Powers LS, and Hunninghake GW. 1999 A phosphatidylcholine-specific phospholipase C regulates activation of p42/44 mitogen-activated protein kinases in lipopolysaccharide-stimulated human alveolar macrophages. J Immunol 162: 3005–3012. [PubMed: 10072552]
24. Sakane F, Imai S, Kai M, Yasuda S, and Kanoh H. 2007 Diacylglycerol kinases: why so many of them? Biochim Biophys Acta 1771: 793–806. [PubMed: 17512245]
25. Merida I, Avila-Flores A, and Merino E. 2008 Diacylglycerol kinases: at the hub of cell signalling. Biochem J 409: 1–18. [PubMed: 18062770]
26. Shulga YV, Topham MK, and Epand RM. 2011 Regulation and functions of diacylglycerol kinases. Chem Rev 111: 6186–6208. [PubMed: 21800853]
27. Zamani A, Decker C, Cremasco V, Hughes L, Novack DV, and Faccio R. 2015 Diacylglycerol Kinase zeta (DGKzeta) Is a Critical Regulator of Bone Homeostasis Via Modulation of c-Fos Levels in Osteoclasts. J Bone Miner Res 30: 1852–1863. [PubMed: 25891971]
28. Liu CH, Machado FS, Guo R, Nichols KE, Burks AW, Aliberti JC, and Zhong XP. 2007 Diacylglycerol kinase zeta regulates microbial recognition and host resistance to Toxoplasma gondii. J Exp Med 204: 781–792. [PubMed: 17371930]
29. Zhong XP, Hainey EA, Olenchock BA, Jordan MS, Maltzman JS, Nichols KE, Shen H, and Koretzky GA. 2003 Enhanced T cell responses due to diacylglycerol kinase zeta deficiency. Nat Immunol 4: 882–890. [PubMed: 12883552]
30. Takeshita S, Kaji K, and Kudo A. 2000 Identification and characterization of the new osteoclast progenitor with macrophage phenotypes being able to differentiate into mature osteoclasts. J Bone Miner Res 15: 1477–1488. [PubMed: 10934646]
31. Behrens EM, Canna SW, Slade K, Rao S, Kreiger PA, Paessler M, Kambayashi T, and Koretzky GA. 2011 Repeated TLR9 stimulation results in macrophage activation syndrome-like disease in mice. J Clin Invest 121: 2264–2277. [PubMed: 21576823]
32. Fukao T, and Koyasu S. 2003 PI3K and negative regulation of TLR signaling. Trends Immunol 24: 358–363. [PubMed: 12860525]
33. Polumuri SK, Toshchakov VY, and Vogel SN. 2007 Role of phosphatidylinositol-3 kinase in transcriptional regulation of TLR-induced IL-12 and IL-10 by Fc gamma receptor ligation in murine macrophages. J Immunol 179: 236–246. [PubMed: 17579043]
34. Murray PJ, Allen JE, Biswas SK, Fisher EA, Gilroy DW, Goerdt S, Gordon S, Hamilton JA, Ivashkiv LB, Lawrence T, Locati M, Mantovani A, Martinez FO, Mege JL, Mosser DM, Natoli G, Saeij JP, Schultze JL, Shirey KA, Sica A, Suttles J, Udalova I, van Ginderachter JA, Vogel SN, and Wynn TA. 2014 Macrophage activation and polarization: nomenclature and experimental guidelines. Immunity 41: 14–20. [PubMed: 25035950]
35. Murray PJ 2017 Macrophage Polarization. Annu Rev Physiol 79: 541–566. [PubMed: 27813830]
36. Misharin AV, Cuda CM, Saber R, Turner JD, Gierut AK, Haines GK 3rd, Berdnikovs S, Filer A, Clark AR, Buckley CD, Mutlu GM, Budinger GR, and Perlman H. 2014 Nonclassical Ly6C(-) monocytes drive the development of inflammatory arthritis in mice. Cell Rep 9: 591–604. [PubMed: 25373902]
37. Macaubas C, Nguyen KD, Peck A, Buckingham J, Deshpande C, Wong E, Alexander HC, Chang SY, Begovich A, Sun Y, Park JL, Pan KH, Lin R, Lih CJ, Augustine EM, Phillips C, Hadjinicolaou AV, Lee T, and Mellins ED. 2012 Alternative activation in systemic juvenile idiopathic arthritis monocytes. Clin Immunol 142: 362–372. [PubMed: 22281427]
38. Zhu Y, Herndon JM, Sojka DK, Kim KW, Knolhoff BL, Zuo C, Cullinan DR, Luo J, Bearden AR, Lavine KJ, Yokoyama WM, Hawkins WG, Fields RC, Randolph GJ, and DeNardo DG. 2017 Tissue-Resident Macrophages in Pancreatic Ductal Adenocarcinoma Originate from Embryonic Hematopoiesis and Promote Tumor Progression. Immunity 47: 323–338. [PubMed: 28813661]
39. Gubin MM, Esaulova E, Ward JP, Malkova ON, Runci D, Wong P, Noguchi T, Arthur CD, Meng W, Alspach E, Medrano RFV, Fronick C, Fehlings M, Newell EW, Fulton RS, Sheehan KCF, Oh ST, Schreiber RD, and Artyomov MN. 2018 High-Dimensional Analysis Delineates Myeloid and Lymphoid Compartment Remodeling during Successful Immune-Checkpoint Cancer Therapy. Cell 175: 1014–1030. [PubMed: 30343900]

40. Kuo D, Ding J, Cohn IS, Zhang F, Wei K, Rao DA, Rozo C, Sokhi UK, Shanaj S, Oliver DJ, Echeverria AP, DiCarlo EF, Brenner MB, Bykerk VP, Goodman SM, Raychaudhuri S, Ratsch G, Ivashkiv LB, and Donlin LT. 2019 HBEGF(+) macrophages in rheumatoid arthritis induce fibroblast invasiveness. Sci Transl Med 11: pii: eaau8587.

41. Shin J, Jang H, Lin J, and Lee SY. 2014 PKCbeta positively regulates RANKL-induced osteoclastogenesis by inactivating GSK-3beta. Mol Cells 37: 747–752. [PubMed: 25256217]

42. Lee SW, Kwak HB, Chung WJ, Cheong H, Kim HH, and Lee ZH. 2003 Participation of protein kinase C beta in osteoclast differentiation and function. Bone 32: 217–227. [PubMed: 12667549]

43. Lim HK, Choi YA, Park W, Lee T, Ryu SH, Kim SY, Kim JR, Kim JH, and Baek SH. 2003 Phosphatidic acid regulates systemic inflammatory responses by modulating the Akt-mammalian target of rapamycin-p70 S6 kinase 1 pathway. J Biol Chem 278: 45117–45127.

44. Channon JY, Leslie CC, and Johnston RB Jr. 1987 Zymosan-stimulated production of phosphatidic acid by macrophages: relationship to release of superoxide anion and inhibition by agents that increase intracellular cyclic AMP. J Leukoc Biol 41: 450–453. [PubMed: 3033115]

45. Olenchock BA, Guo R, Carpenter JH, Jordan M, Topham MK, Koretzky GA, and Zhong XP. 2006 Disruption of diacylglycerol metabolism impairs the induction of T cell anergy. Nat Immunol 7: 1174–1181. [PubMed: 17028587]

46. Olenchock BA, Guo R, Silverman MA, Wu JN, Carpenter JH, Koretzky GA, and Zhong XP. 2006 Impaired degranulation but enhanced cytokine production after Fc epsilonRI stimulation of diacylglycerol kinase zeta-deficient mast cells. J Exp Med 203: 1471–1480. [PubMed: 16717114]

47. Cremasco V, Graham DB, Novack DV, Swat W, and Faccio R. 2008 Vav/Phospholipase Cgamma2-mediated control of a neutrophil-dependent murine model of rheumatoid arthritis. Arthritis Rheum 58: 2712–2722. [PubMed: 18759305]

48. Yang Z, Yan H, Dai W, Jing J, Yang Y, Mahajan S, Zhou Y, Li W, Macaubas C, Mellins ED, Shih CC, Fitzpatrick JAJ, and Faccio R. 2019 Tmem178 negatively regulates store-operated calcium entry in myeloid cells via association with STIM1. J Autoimmun 101: 94–108. [PubMed: 31018906]

Key points

1. 1) *Dgkζ* deficiency protects from the induction of inflammatory arthritis.
2. 2) *Dgkζ* deficiency limits activation of pro-inflammatory macrophages.
3. 3) *Dgkζ* deficiency reduces phosphorylation of STAT1 and STAT3 in activated macrophages.

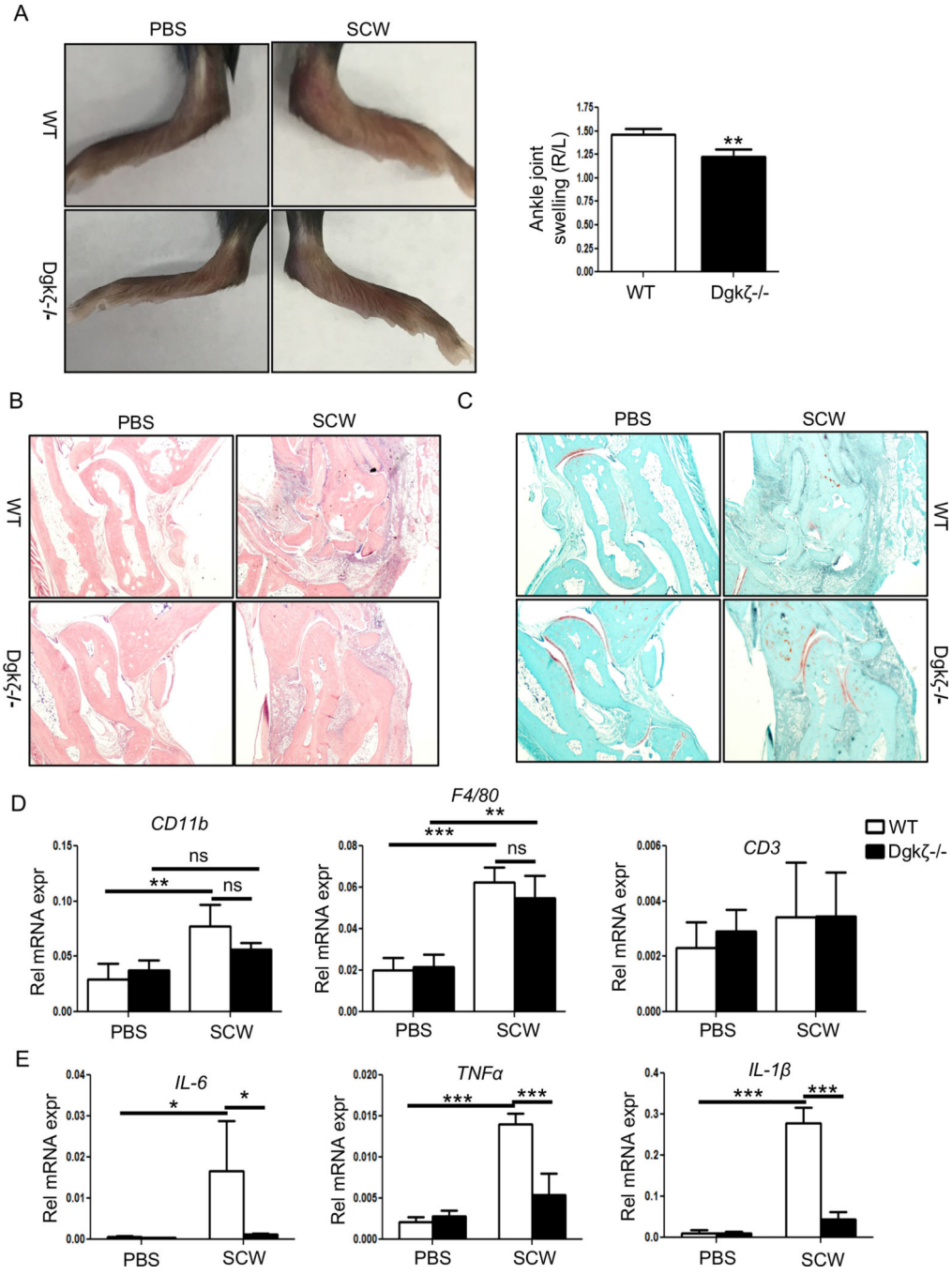

Figure 1. *Dgkζ* deficiency ameliorates SCW-induced arthritis

C57Bl/6 WT and *Dgkζ*-/- mice were injected with 25 μg of SCW fragments in the right ankle while the left ankle injected with PBS served as control, and the animals were euthanized 3 days later. (A) Representative images of ankles from WT and *Dgkζ*-/- mice injected with PBS or SCW fragments. The joint swelling in WT and *Dgkζ*-/- mice was determined by caliper measurement of the injected ankles. (B) Representative histological sections of ankle joints stained with H&E showing presence of immune infiltrates. (C) Representative images of ankle joints stained with safranin O depicting cartilage destruction.

(D-E) RT-PCR analysis for the immune markers CD11b, F4/80 and CD3 (D) and inflammatory cytokines IL-6, TNFα and IL-1β (E) in the ankle joints of WT and *Dgkζ* deficient mice. Bars in Figure A and D-E (n= 3 mice/group) represent mean and SD. Statistical significance was determined by two-tailed Student's t test or two-way ANOVA for multiple comparison. * $p<0.05$, ** $p<0.01$, *** $p<0.001$.

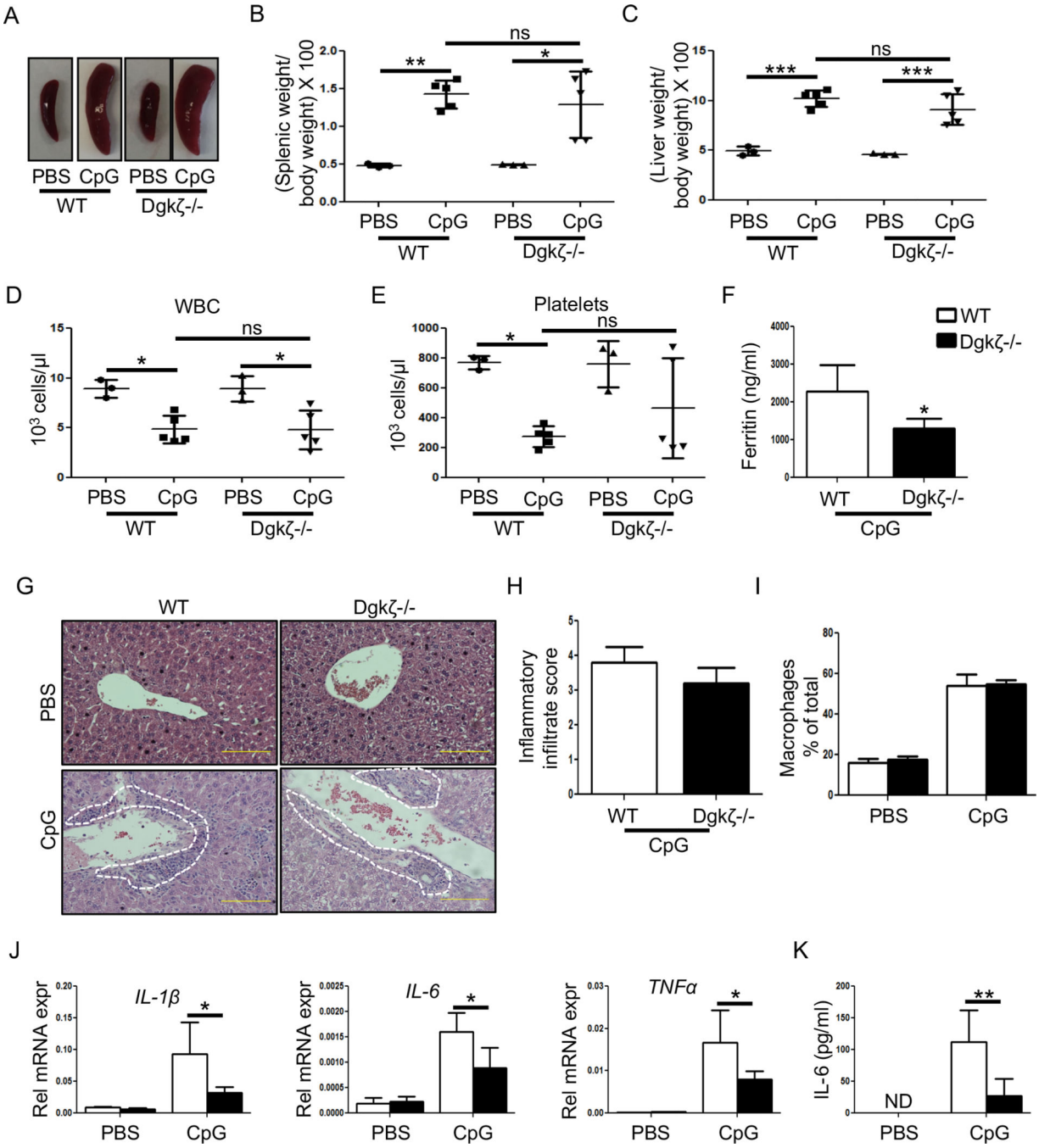

Figure 2. Loss of *Dgkζ* attenuates inflammatory cytokine production in the TLR9 induced-CSS model

C57Bl/6 WT and *Dgkζ*-/- mice were injected with either PBS or CpG (50 μg) every other day for 8 days. The mice were euthanized within 24 hr after the last CpG injection for analysis. (A-B) Representative images of spleen size (A) and measurements of spleen weight in WT and *Dgkζ-/-* mice injected with PBS or CpG to induce CSS (B). (C) Development of hepatomegaly determined by measuring the ratio of liver weight to body weight x 100. (D-E) WBC (D) and platelet (E) counts in mice with CSS. (F) Serum ferritin levels from WT and *Dgkζ-/-* mice measured on day 9 after CpG-induced CSS. (G)

Representative H&E stained liver sections highlighting presence of inflammatory infiltrates (indicated by white dotted lines). (H) The liver inflammatory infiltrate score determined by assessing the extent of inflammatory cells around the veins and parenchyma, with 0 being the lowest and 4 being the highest given score. (I) The quantification of macrophages in the liver of WT and *Dgkζ* deficient mice determined by FACS in PBS controls and after CpG-induced CSS. (J) The transcripts levels of inflammatory cytokines measured in the liver of WT and *Dgkζ* deficient mice in PBS controls and after CpG-induced CSS. (K) IL-6 levels in the blood analyzed by performing ELISA in the serum. Individual symbols in Figure B-E represent 1 mouse with horizontal lines representing the mean values. Bars in Figures F-K (n= 5–9 mice/group) represents mean and SD. Statistical significance was determined by two-tailed Student's t test or two-way ANOVA for multiple comparison. * $p<0.05$, ** $p<0.01$, *** $p<0.001$.

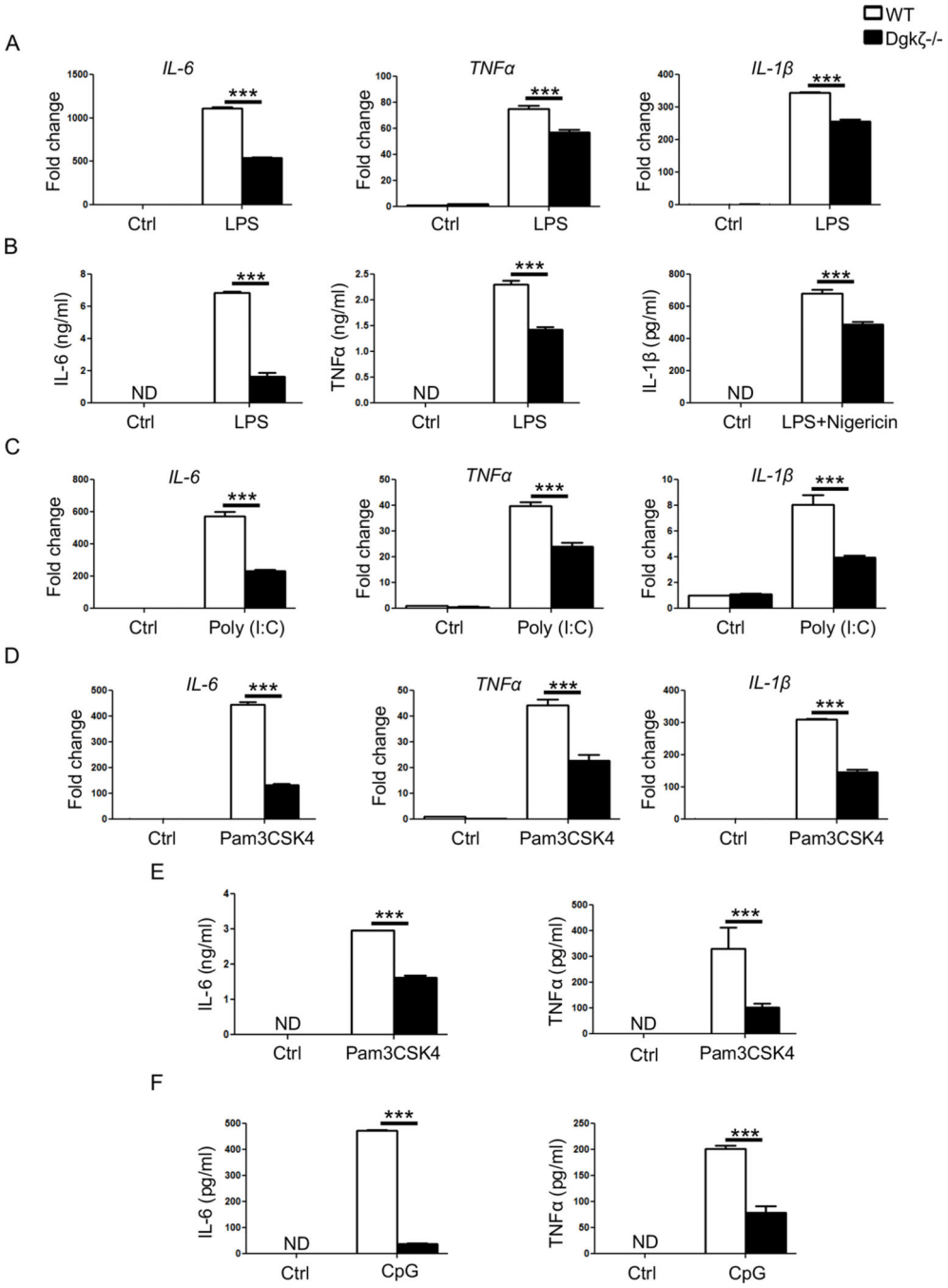

Figure 3. Decreased cytokine production in macrophages from *Dgkζ*-/- mice

(A) RT-qPCR analysis of inflammatory cytokines in BMMs derived either from WT or *Dgkζ-/-* mice and stimulated with 100 ng/ml of LPS for 4 hr. Data are expressed as fold change in gene expression in comparison to unstimulated WT BMMs. (B) Levels of IL-6 and TNFα measured by ELISA in the supernatant of BMMs stimulated with 100 ng/ml of LPS for 24 hr. IL-1β protein levels determined after stimulation with LPS (100 ng/ml) for 2 hrs followed by 7.5 μM nigericin for 15 mins. (C-D) RT-qPCR analysis of IL-6, TNFα and IL-1β in BMMs from WT or *Dgkζ-/-* mice stimulated for 4 hr with 40 μg/ml of poly (I:C)

(C) or 50 ng/ml of pam3CSK4 (D). Data are expressed as fold change in gene expression in comparison to unstimulated WT BMMs. (E-F) IL-6 and TNFα measured by ELISA in the supernatant of BMMs from WT and *Dgkζ-/-* mice stimulated with 50 ng/ml of pam3CSK4 (E) or 1 μM of CpG (F) for 24 hr. Statistical significance was determined by two-way ANOVA. * $p<0.05$, ** $p<0.01$, *** $p<0.001$.

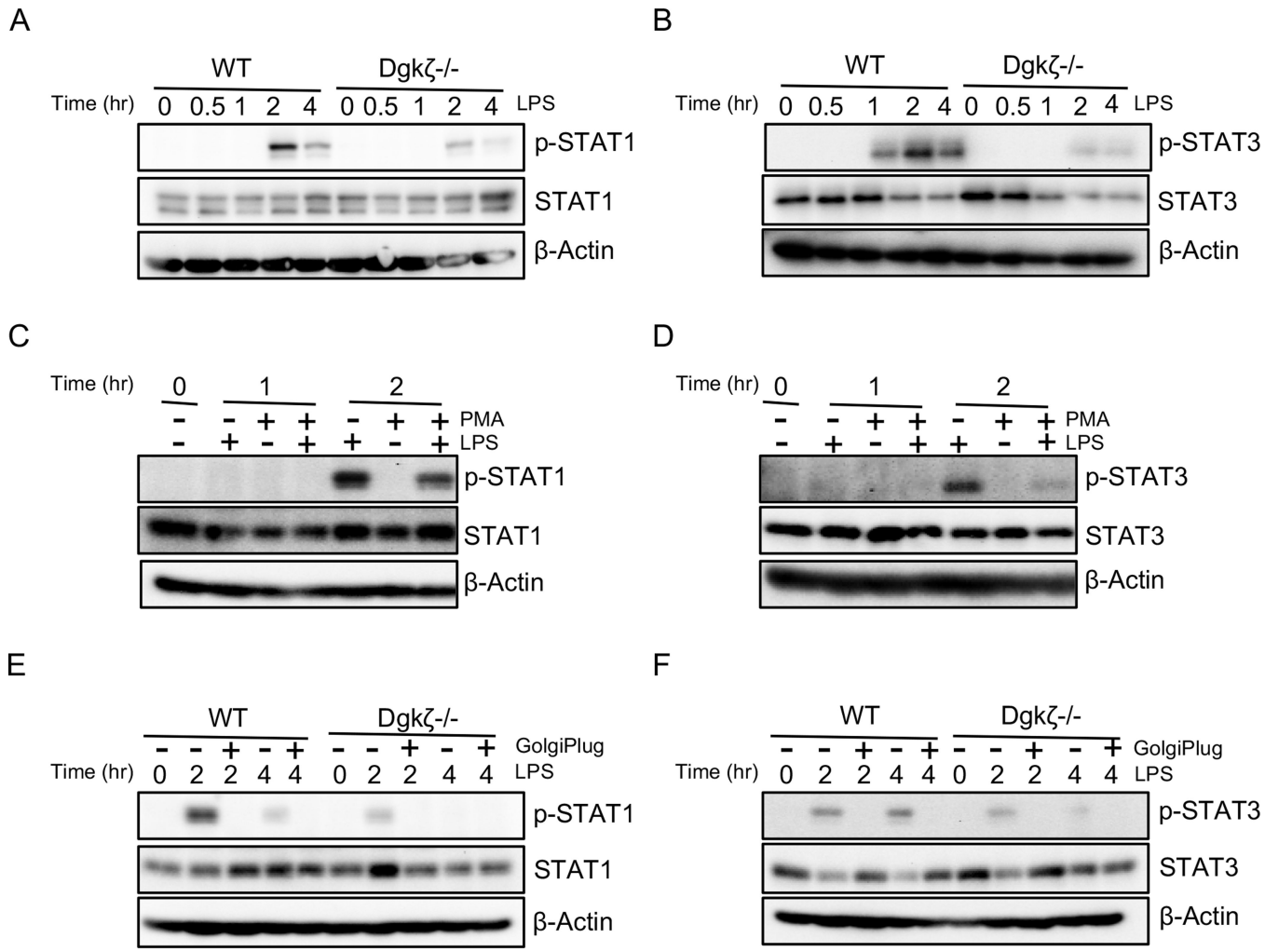

Figure 4. *Dgkζ* deficiency reduces STAT1/3 activation in macrophages

(A-B) BMMs from WT or *Dgkζ*-/- mice stimulated with LPS for indicated time points and subjected to western blot analysis for phospho-STAT1 and total STAT1 (A) and phospho-STAT3 and total STAT3 (B). (C-D) Western blot analysis of indicated proteins in WT BMMs treated either with 100 ng/ml LPS, 100 nM PMA or LPS and PMA together for indicated time points. (E-F) BMMs from WT or *Dgkζ*-/- mice stimulated with 100 ng/ml LPS alone or with LPS in the presence of 1 μl/ml GolgiPlug for indicated time and blotted for phospho-STAT1 and total STAT1 (E) and phospho-STAT3 and total STAT3 (F). β-Actin was used as a loading control.

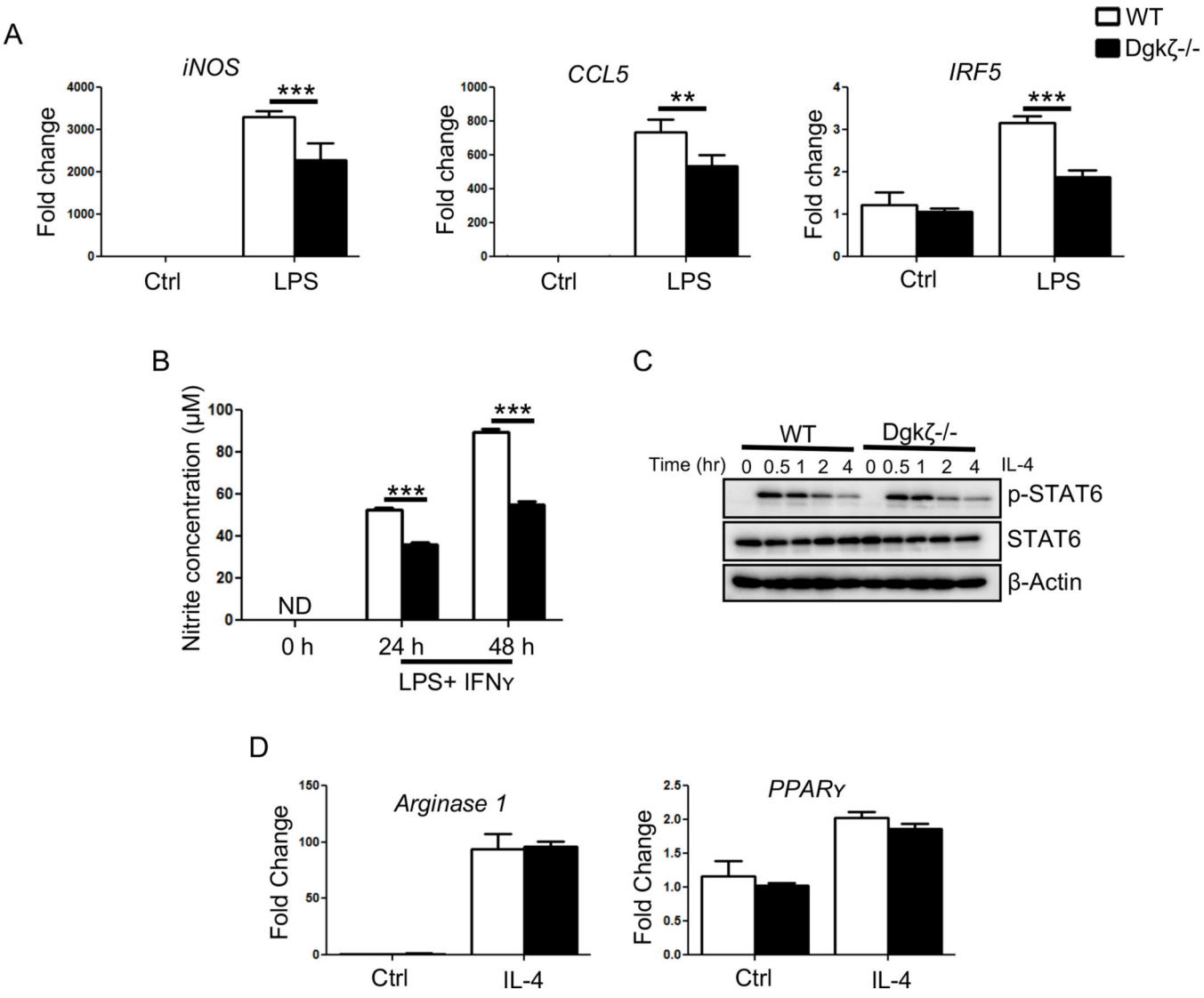

Figure 5. Loss of *Dgkζ* limits M1 macrophage polarization

(A) The transcript levels of iNOS, CCL5 and IRF5 determined by RT-qPCR analysis in BMMs stimulated with 100 ng/ml of LPS for 4 hr. Data are expressed as fold change in gene expression in comparison to unstimulated WT BMMs. (B) Nitrite concentration in the supernatant of BMMs stimulated with LPS (100 ng/ml) and IFNγ (100 ng/ml) determined by Griess assay. (C) BMMs stimulated with IL-4 for indicated time and subjected to western blot analysis for phospho-STAT6 and STAT6. β-Actin was used as a loading control. (D) RT-qPCR analysis of Arginase 1 and PPARγ in BMMs derived either from WT or *Dgkζ-/-* mice and stimulated with 50 ng/ml of IL-4 for 12 hr. Data are expressed as fold change in gene expression in comparison to unstimulated WT BMMs. Statistical significance was determined by two-way ANOVA. * $p<0.05$, ** $p<0.01$, *** $p<0.001$.

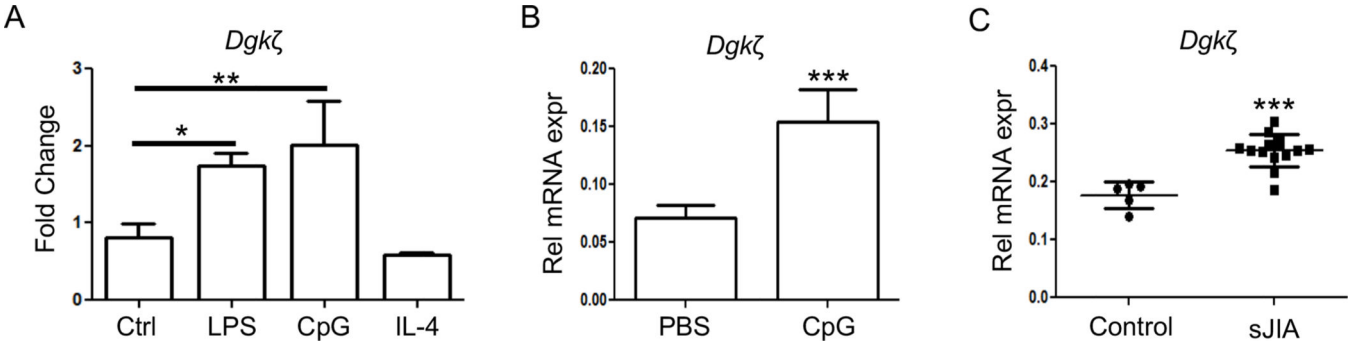

Figure 6. Inflammatory conditions induce *Dgkζ* expression

(A) Expression of Dgkζ was determined by RT-qPCR in BMMs left either unstimulated (Ctrl) or stimulated with LPS (100 ng/ml), CpG (1 μM) and IL-4 (50 ng/ml) for 12 hr. (B) mRNA expression of Dgkζ determined in the liver of mice that were given repeated injections of PBS or CpG to induce CSS (n=5/ group). (C) mRNA expression of Dgkζ measured in BMMs treated with either healthy control or sJIA plasma for 12 hr. Bars in Figure A and B represents mean and SD while each symbol in Figure C represent 1 individual with horizontal lines representing the mean values. Statistical significance was determined using unpaired t-test or one-way ANOVA. * $p<0.05$, ** $p<0.01$, *** $p<0.001$.